Rinne, Marja; Aromaa-Stubb, Riina; Elomaa, Heini; Porvali, Antti; Lundström, Mari

Evaluation of hydrometallurgical black mass recycling with simulation-based life cycle assessment

Published in:
International Journal of Life Cycle Assessment

DOI:
10.1007/s11367-024-02304-y

Published: 01/09/2024

Document Version
Publisher's PDF, also known as Version of record

The International Journal of Life Cycle Assessment (2024) 29:1582–1597
https://doi.org/10.1007/s11367-024-02304-y

CARBON FOOTPRINTING

Evaluation of hydrometallurgical black mass recycling with simulation-based life cycle assessment

Marja Rinne[1] · Riina Aromaa-Stubb[1] · Heini Elomaa[2] · Antti Porvali[3] · Mari Lundström[1]

Received: 8 March 2023 / Accepted: 22 March 2024 / Published online: 3 May 2024

Abstract

Purpose The recycling of lithium-ion batteries is an emerging field faced with the challenge of recovering more than the most valuable elements from the batteries. While the literature presents many innovative approaches to the problem, an overview of the technical and environmental prospects of hydrometallurgical black mass recycling remains crucial. The goal was to analyze the impacts of a black mass process flowsheet and suggest ways to further reduce the impacts of battery recycling.

Methods The flowsheet was drafted from the literature by combining both state-of-the-art and experimentally demonstrated unit processes by starting with the leaching system, where reductive leaching is performed using only the copper and iron impurities already present in the black mass. The process targeted copper, manganese, cobalt, nickel, and lithium recovery, and three scenarios for manganese recovery were investigated. The flowsheet was simulated using HSC Sim software, and the mass and energy balances were adapted into internally consistent life cycle inventories. The scope was "gate-to-gate" in Europe and CML methodology was used for impact assessment.

Results and discussion Assuming that mechanical pre-treatment carries more environmental benefits than burdens, the results indicated that hydrometallurgical black mass recycling had a tentatively lower environmental footprint compared to virgin raw materials in all impact categories except ozone depletion, the results indicated that hydrometallurgical black mass recycling had a tentatively lower environmental footprint compared to virgin raw materials in all impact categories except ozone depletion. Sulfuric acid and neutralizing chemicals were among the most significant contributors to the impacts, and therefore further analysis was conducted based on an experimental study on low acid leaching with a low (< 0.5 M) initial sulfuric acid concentration instead of the baseline 2 M. This reduced the impacts by approximately 30–40% in all categories by decreasing downstream chemical consumption, and more significantly decreased ozone depletion. The challenges and opportunities for further process improvement were also considered.

Conclusions The study highlights the importance of process optimization to improve the environmental sustainability of battery chemical production, but also revealed critical research gaps in the experimental literature. Rather than focusing on a single unit process, experimental black mass recycling research should aim at finding solutions that are optimal for the up- and downstream units, such as minimization of aluminum in the black mass and acid consumption.

Keywords Battery recycling · Environmental impacts · Flowsheet simulation · Process optimization · Cathode materials · Leaching

Communicated by Andrea J Russell-Vaccari.

✉ Mari Lundström
mari.lundstrom@aalto.fi

[1] School of Chemical Engineering, Department of Chemical and Metallurgical Engineering, Aalto University, Vuorimiehentie 2, P.O. Box 16200, FI-00076 Aalto, Finland

[2] Metso Finland Oy, Rauhalanpuisto 9, FI-02231 Espoo, Finland

[3] VTT Technical Research Centre of Finland Ltd, FI-02044 VTT, Finland

1 Introduction

The electrification of transport is a key pathway in the transition to a low carbon economy (Keramidas et al. 2020). Several studies have demonstrated that, depending on the electricity supply mix, electric vehicles (EVs) can significantly reduce greenhouse gas (GHG) emissions over conventional internal combustion engine vehicles (ICEVs) during their use phase (Bauer et al. 2015; Bicer and Dincer 2018; Faria et al. 2013); however, there is much uncertainty

regarding the indirect environmental impacts of EV batteries in the manufacturing and end-of-life (EOL) stages. As several authors (Mohr et al. 2020; Rajaeifar et al. 2021) have observed, the EOL stage of the battery has frequently been omitted from the system boundary due to the large number of unknowns and data gaps. Nevertheless, the efficient recycling of automotive lithium-ion (Li-ion) batteries is recognized as a critical measure to mitigate resource constraints and decrease the environmental risks of disposal (Harper et al. 2019).

The most typical cathode materials in batteries used in EVs are lithium nickel manganese cobalt oxide (NMC, $LiNi_xMn_yCo_{1-x-y}O_2$), lithium nickel cobalt aluminum oxide (NCA, $LiNi_{0.8}Co_{0.15}Al_{0.05}O_2$), and lithium iron phosphate ($LiFePO_4$), of which NMC has dominated the market to date. Lithium cobalt oxide ($LiCoO_2$, LCO) is not relevant to EVs, but it remains important for consumer electronics (Chu et al. 2022). The feedstock of Li-ion batteries to recycling has been limited, and therefore the recycling industry has mainly targeted the recovery of valuable cobalt, nickel, copper, and recently also lithium, while other components like manganese, electrolyte, and graphite have usually been lost to waste fractions. Dedicated and tailored Li-ion recycling processes are currently slowly emerging, but the heterogeneity of waste batteries both in terms of cathode chemistries and the lack of standardized module and cell design makes this a challenging prospect for process development (Thompson et al. 2020). Hydrometallurgical treatment of active material powder obtained by mechanically pre-treating crushed Li-ion batteries, so-called black mass, has gained momentum because the processes can separate and recover pure metals and metal salts, including elements that are currently lost (Yao et al. 2018). The flowsheets are complex, however, and the consumption of energy and reagents may be high.

Although battery recycling is generally viewed as environmentally advantageous compared to virgin mining, life cycle assessment (LCA) studies that address the EOL stage have reached a wide spectrum of conclusions about the processes involved. Direct recycling of cathodes, hydrometallurgical processes, and pyrometallurgical processes have been under consideration (Ciez and Whitacre 2019; Jiang et al. 2022; Kallitsis et al. 2022; Mohr et al. 2021; Rajaeifar et al. 2021; Rinne et al. 2021). The as yet non-commercial and technologically immature direct recycling processes appear to have the most benefits regardless of the cathode chemistry, according to some studies (Ciez and Whitacre 2019; Jiang et al. 2022). Hydrometallurgical and possibly pyrometallurgical processes appear to mitigate the impacts for cobalt and nickel bearing cathode chemistries (Blömeke et al. 2022; Rajaeifar et al. 2021), but not for lithium iron phosphate (LFP, $LiFePO_4$) (Ciez and Whitacre 2019; Mohr et al. 2021; Rajaeifar et al. 2021). Quan et al. (2022), however, predicted that the hydrometallurgical processing of LFP would outperform direct recycling, which contradicts the abovementioned findings.

Although it has been argued by Mohr et al. (2020) that studying the impacts of battery EOL stage using mixed battery material feeds limits the usefulness of the results, it can also be stated that a process-centric approach can be invaluable for the development and optimization of flowsheets. Rajaeifar et al. (2021), for instance, determined that mechanical pre-treatment alone can lead to meaningful improvement of the pyrometallurgical process impacts through the recovery of aluminum, which is not recovered in the current processes. The benefit of aluminum recovery is supported by the findings of Kallitsis et al. (2022) and Rinne et al. (2021), and the overall benefit of mechanical pre-treatment in reducing downstream process complexity has been demonstrated by Blömeke et al. (2022). Cao et al. (2023) also suggest that the recovery of some co-products can unduly increase the impacts of recycling due to the increased flowsheet complexity.

Furthermore, the simplification of complex processes into generic "mechanical," "pyrometallurgical," and "hydrometallurgical" processes is misleading, since all types of processes may be operated under a variety of different conditions and flowsheet configurations. This applies particularly to hydrometallurgical battery recycling, which has yet to mature on industrial scale, unlike pyrometallurgical processing in Europe (Latini et al. 2022). While it remains to be seen what types of hydrometallurgical methods will be widely applied in the industry in the future, the current flowsheets, practices, and regulations provide foresight on how the field is evolving. Rigorous process simulation can be an invaluable tool for generating data on interesting process routes that are not yet in industrial scale, since it has been shown to be more accurate than piloting in some instances (Tsalidis and Korevaar 2022). The main value in detailed process modeling is that it can overcome the "black box" nature of processes and provide transparency to LCA practitioners.

To that end, the goal of this study was to apply process simulation and LCA to study the impacts of a potential hydrometallurgical black mass process that uses acidic sulfate media in the absence of external reducing agents. Process simulation using Metso's (2023) HSC Sim 10 software was used to obtain high resolution life cycle inventory (LCI) data on the investigated flowsheets and process conditions, and the impact assessment (LCIA) phase was conducted with Sphera's GaBi using data from the Ecoinvent 3.8 database. Detailed process modeling and LCA were coupled in this study to assess the connections between model inputs and parameters and the environmental impacts, and ultimately to inform process development of the most effective ways to reduce the burdens from recycling.

2 Materials and methods

The present work consists of (1) goal and scope definition, (2) life cycle inventory analysis, (3) impact assessment, and (4) interpretation stages, as outlined in ISO 14040:2006/A1:2020:en (2020). The study is prospective, and process simulation and chemical engineering knowledge were used for inventory analysis and interpretation of the study.

2.1 Goal and scope definition

The goal of the study was to investigate the *prospective* hydrometallurgical processing of black mass recycling in high resolution. The purpose was to recognize the most effective ways to reduce the impacts of hydrometallurgical processing by evaluating the connections between different process parameters and inventory flows. The analysis was conducted gate-to-gate, starting with the leaching of black mass and ending in the recovery of the target valuable metals: lithium, manganese, cobalt, and nickel. The study is set in Europe and the background was modeled accordingly.

The energy and mass balances were modeled with Metso's (2023) HSC Sim v. 10.0.8.5 software using experimentally determined data on process parameters, yields, dependencies, and chemical behavior, which was collected from the literature. The detailed simulation also enabled the assessment of how the LCA results are affected by changes in the parameters, feed material, or parts of the flowsheet. The LCI generated this way is internally cohesive. GaBi v. 10.5.0.78 (Sphera 2023) was used in the impact assessment and background data was obtained from Ecoinvent v. 3.8, using "allocation at the point of substitution" (APOS) models (Ecoinvent 2021).

2.1.1 System boundaries

The analysis was conducted gate-to-gate and includes the steps in the hydrometallurgical processing of active material powder, starting from leaching and ending with the metal recovery stages. The study therefore excludes upstream pre-treatment in accordance with the goal statement and, in turn, the hydrometallurgical process was assessed in a high level of detail.

The pre-treatment consists of an array of different units to concentrate the materials into different fractions based mostly on physical characteristics. Crushing and sieving alone can, for instance, be used to separate most of the copper and aluminum foils from the cathode and anode powder based on their larger particle size. It is noteworthy that a large share of the recycling benefits appears to originate from the recovery of copper and aluminum (Kallitsis et al. 2022; Rajaeifar et al. 2021; Rinne et al. 2021), but this is excluded from the present work. The system boundaries and the investigated flowsheets are presented in Fig. 1.

Three flowsheet formulations (flowsheets *FS1*, *FS2*, and *FS3*) and two types of leaching conditions (baseline and low acid, *LA*) were modeled using experimentally determined process parameters, reactions, and extractions. The simulated flowsheet is not operated industrially in the current form, but the individual units, i.e., reductive leaching, copper cementation, and lithium carbonate crystallization, are established processes with the exception of manganese purification by solvent extraction (SX), which has been proven on lab scale (Peng et al. 2019). The hydrometallurgical flowsheet was formulated mainly based on the state-of-the-art practices in the industry, with the desired final products being manganese dioxide, hydrated cobalt sulfate, hydrated nickel sulfate, and lithium carbonate. Copper powder, which is produced by cementation, is re-used as a reducing agent in leaching. The goal of the process is to produce battery-grade chemicals for cathode materials; therefore, the purities were assessed with the simulation to evaluate further refining requirements.

The black mass analyses used in the study were obtained from Liu et al. (2019) and presented in Table 1. The batteries were industrially pre-treated by crushing, magnetic separation, and sieving to obtain < 0.125 mm black mass. It should be stressed that the sieve size is smaller than in typical industrial processing to reduce the heterogeneity of the material, which is crucial for studying the leaching phenomena on laboratory scale. Industrial black mass tends to contain more copper and aluminum, which have a coarser particle size than the active materials after comminution (Chernyaev et al. 2022; Porvali et al. 2019). The chemical analysis was converted into a material composition in terms of individual oxides and other materials as in the earlier study by Rinne et al. (2021) by balancing the analysis with carbon. Trace quantities of other impurities such as polymers, fluoride, and organics may be present, but they were not included in the simulation.

Although the analysis is not fully representative, the process model can be used to assess the minimum impurity content where the material may be considered self-reducing, i.e., how much copper, iron, and aluminum is required to avoid the need for external reducing agents. By estimation, 1 kg of black mass with the composition used here (60% carbon, 39% active metal oxides) corresponds to approximately 3 kg battery cells containing 0.5 kg copper.

The black mass used is cobalt rich, but the current and future commercial EVs are powered by other types of cathodes, such as NMC and NCA. NMC has become the dominant technology (Schade et al. 2022). The substitution of cobalt with nickel is a key trend in the development of NMC batteries due to lower dependence on high-cost cobalt

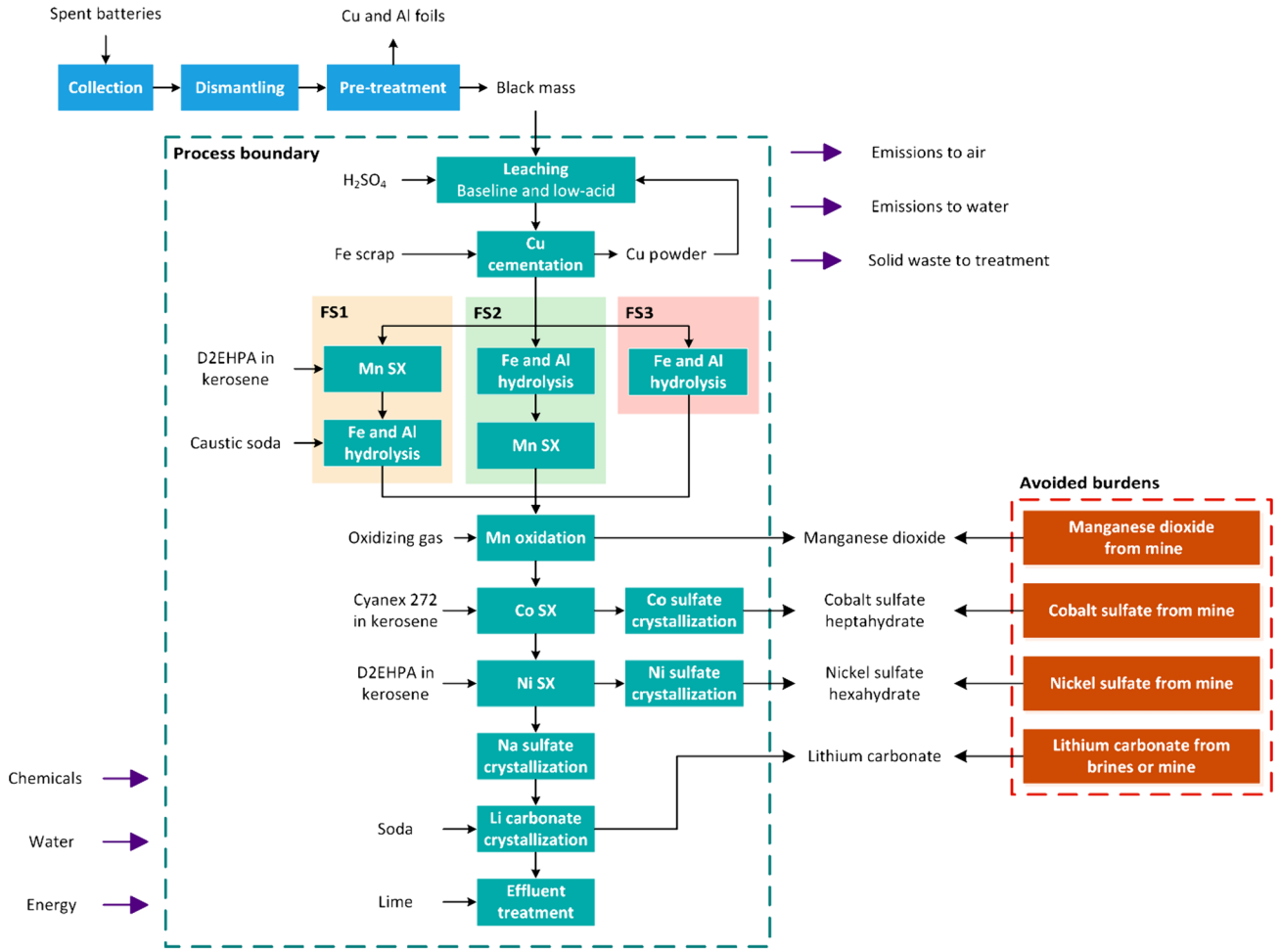

Fig. 1 The system boundary and process schematic marked with a dashed line. Not all in- and outflows are included. The scenarios *FS1*, *FS2*, and *FS3* are highlighted with yellow, green, and red backgrounds, respectively

on top of improved specific energy and capacity (Andre et al. 2015). This has led to the development and increased use of high-nickel NMC cathodes, such as NMC532 (50% Ni, 30% Mn, 20% Co) and NMC811 (80% Ni, 10% Mn, 10% Co). The process was designed to recover each of the valuables in NMC, and the sensitivity of the model to different NMC feeds was assessed.

The simulation model relies on HSC Sim's hydrometallurgical reaction models, where the output of a unit is defined using chemical reactions, phase distributions, and inputs. Therefore, the chemical reactions occurring in each of the units needed to be determined to obtain chemical consumptions and the solution composition that would affect the next unit.

Table 1 Chemical analysis of the cobalt-rich black mass obtained from Liu et al. (2019), modified into a material composition balanced with graphite (carbon, C) and converted to NMC-rich mass

Element	**Li**	**Co**	**Ni**	**Mn**	**Cu**	**Al**	**Fe**
mg/g	39.7	207.9	29.9	18.7	4.0	5.4	3.70
Material	**$LiCoO_2$**	**$LiNiO_2$**	**$LiMnO_2$**	**Cu**	**Al**	**Fe**	**C**
Co-rich (wt.%)	31.21	4.97	2.65	0.40	0.54	0.37	59.86
NMC111 (wt.%)	12.97	12.94	12.44	0.40	0.54	0.37	60.34
NMC532 (wt.%)	7.79	19.43	11.21	0.40	0.54	0.37	60.26
NMC811 (wt.%)	3.90	31.09	3.74	0.40	0.54	0.37	59.97

The investigated hydrometallurgical process uses no external reducing agents, such as hydrogen peroxide, to dissolve the active materials, but instead relies on metallic impurities that are already present in most industrial black masses: copper, iron, and aluminum. The leaching systems have been discussed in detail in the works of Porvali et al. (2020a, b). Furthermore, Chernyaev et al. (2021a) validated the fact that industrial black mass that dissolved iron (II) was beneficial in a leaching system containing copper and aluminum foils.

In the absence of a reductant, the dissolution of active cathode materials ($LiMeO_2$) proceeds according to reaction (1) (Nan et al. 2005). In the presence of dissolved ferrous iron, reaction (2) may also occur. It was estimated that approximately 60% of the lithium metal oxides dissolve directly in acid since approximately 60–80% of cobalt typically dissolves from LCO without a reducing agent. The rest of the oxides were assumed to dissolve according to reaction (2). The progress affects the consumption of acid and the behaviour of copper and iron in the system.

$$4LiMeO_2 + 6H_2SO_4 \rightarrow 2Li_2SO_4 + 4MeSO_4 + 6H_2O + O_2(g) \quad (1)$$

$$2LiMeO_2 + 4H_2SO_4 + 2FeSO_4 \rightarrow Li_2SO_4 + 2MeSO_4 + Fe_2(SO_4)_3 + 4H_2O \quad (2)$$

Metallic iron present in the black mass dissolves in acid according to reaction (3). A high concentration of iron in the solution is undesirable from the perspective of the subsequent solution purification (Chernyaev et al. 2021b), and Porvali et al. (2020a) determined the minimum consumption of iron able to efficiently dissolve $LiCoO_2$ in a synthetic system. The presence or addition of metallic copper can remedy this, as ferric ions (Fe^{3+}) can be regenerated to ferrous (Fe^{2+}) by reaction (4). Chernyaev et al. (2022) estimated that 78% of ferric iron regenerates to ferrous in contact with copper, while copper dissolves and needs to be recovered in the later stages of the process. Reaction (4) was thus set to proceed 78%, which indicates that more than a stoichiometric quantity of copper is required. Oxygen generated in reaction (1) was assumed to not oxidize any metals or dissolved species, but there is a possibility that side reactions could occur.

$$Fe + H_2SO_4 \rightarrow FeSO_4 + H_2(g) \quad (3)$$

$$Fe_2(SO_4)_3 + Cu \rightarrow CuSO_4 + 2FeSO_4 \quad (4)$$

The dissolution of cathode materials in an Fe-catalyzed system may thus be described by reaction (5). Copper is consumed at stoichiometric quantities or above, whereas a small (0.11 mol Fe per 1 mol $LiCoO_2$) amount of iron is needed as a catalyst for leaching since it continuously regenerates in contact with solid copper (Porvali et al. 2020a).

$$2LiMeO_2 + 4H_2SO_4 + Cu \xrightarrow{Fe(II, III)} Li_2SO_4 + 2MeSO_4 + CuSO_4 + 4H_2O \quad (5)$$

There is some indication that a similar mechanism benefits the dissolution of NMC, although no detailed kinetic studies have been performed. Joulié et al. (2017), for instance, showed that NMC leaching is enhanced by the addition of copper and aluminum foils. Guimarães et al. (2022) claimed to have leached NMC811 black mass in sulfuric acid "in the absence of a reducing agent," but the black mass composition would rather suggest that copper and aluminum in the waste provided reducing power to the system, which demonstrates that some black masses can be self-reducing. NMC was presumed to dissolve at a similar rate as LCO in the current work.

The leaching step is acid-consuming. The dissolution of 1 kg active NMC material consumes 1.5–2.1 kg sulfuric acid without considering the side reactions. The leaching step has traditionally been studied at high excess acidities, which affects the downstream processing. Porvali et al. (2020b) investigated the leaching of LCO material at an atypically low initial solution acidity (0.34 M sulfuric acid) in the iron-copper system and achieved 92% cobalt extraction after 2 h. Hence, baseline conditions with initial sulfuric acid concentrations of 2 M and ~ 0.5 M were selected for further evaluation based on the work of Porvali et al. (2020a, 2020b).

A key process design consideration was the efficient use of copper and iron in the process to avoid the need for external reducing agents even with varying black mass compositions. Copper is most typically separated from acidic sulfate solutions either by the solvent extraction-electrowinning route, sulfide precipitation, or cementation. Cementation using iron powder was selected as the most straightforward way to recycle the copper product back to the leaching step. The cementation process also introduces dissolved iron into the solution, which may be used to provide iron (II) ions for the leaching step.

After copper cementation, iron and aluminum are removed from the solution by precipitation and manganese is precipitated as manganese (IV) oxide. Iron electrochemically oxidizes before manganese, which is why iron needs to be separated from the solution before the manganese precipitation step. Three flowsheet sequences are proposed for the technical and environmental review of iron and aluminum removal and manganese recovery: co-extraction and selective stripping (flowsheet 1, *FS1*), iron removal followed by manganese solvent extraction (flowsheet 2, *FS2*), and iron removal followed by direct manganese oxidation (flowsheet 3, *FS3*). In each of the flowsheets manganese recovery is conducted by oxidative precipitation from the generated solution, and the other steps—leaching, copper recovery, cobalt and nickel recovery, lithium recovery, effluent

treatment—are simulated identically in all the scenarios, and the downstream effects of flowsheet changes are seen from the models.

The first option for the separation of iron and aluminum before manganese oxidation was proposed by Peng et al. (2019), who co-extracted manganese, iron, and aluminum with D2EHPA (optimal conditions 1:1 O/A ratio, pH 3.2, 40 vol% D2EHPA in kerosene), which was tried in *FS1*. Co-extracted cobalt, lithium, and nickel can be efficiently scrubbed out of the organic phase with dilute manganese sulfate solutions, which is supported by the findings of Vieceli et al. (2021) using iron and aluminum-depleted solutions. As in the work of Peng et al. (2019), manganese is separated from the aluminum and iron in the organic phase by selective stripping with 0.5 M sulfuric acid solution, due to the stronger metal-D2EHPA complex formed by the impurities. Forty percent of the aluminum and a negligible share of iron are stripped into the manganese-rich solution, which is then subjected to oxidative precipitation of manganese. The raffinate, containing cobalt, nickel, and lithium, is pumped forward to cobalt extraction. The organic phase is treated for iron and aluminum removal with concentrated (6 M) hydrochloric acid solution, although this is a possible fire hazard in industrial settings.

If the amount of iron and aluminum in the feed solution to solvent extraction was low, this could be feasible, but due to the potential technical problems, the alternative processing strategy of *FS2* was considered. In *FS2*, iron and aluminum are first removed as hydroxides by neutralizing the solution to pH 4 with caustic soda (Chernyaev et al. 2021b). A high aluminum content in the solution was observed to lead to increased losses of valuable metals in the solution, and careful pH control is necessary to avoid excessive co-precipitation of cobalt, nickel, manganese, and lithium; at higher pH, more valuable metals are lost to the iron-aluminum hydroxide waste stream. The solution is subjected to manganese solvent extraction with D2EHPA, and organic scrubbing with hydrochloric acid is avoided. The cobalt-, nickel-, and lithium-rich raffinate is pumped to cobalt extraction and the purified manganese solution to manganese oxidation.

A far simpler approach to iron-manganese treatment would be to remove iron and aluminum by pregnant leaching solution (PLS) neutralization and the consequent direct precipitation of manganese without solvent extraction, as in *FS3*. Zhang and Singh (2002) successfully precipitated manganese dioxide from simulated laterite leaching solutions with 0.01 M manganese, 0.1 M cobalt, and 0.1 M nickel using oxygen and sulfur dioxide gas mixtures. In the precipitation process, oxygen is the oxidant, but the reaction is slow in the absence of sulfur dioxide (6 vol%), which acts as a catalyst. In addition to the gas mixture, less cost-effective oxidants such as potassium permanganate, ammonium persulfate, and ozone have been used in the past for manganese recovery in the literature (Zhang and Cheng 2007). Appreciable selectivity for manganese was obtained at pH 3, where only 0.7% cobalt and < 0.2% nickel precipitated.

After iron and aluminum removal and manganese recovery, cobalt and nickel are recovered from the purified PLS by solvent extraction and metal sulfate crystallization from the purified solutions. After nickel extraction, the only valuable metal in the raffinate is lithium, which is crystallized as lithium carbonate. Energy intensive water evaporation is required due to the high solubility of the carbonate product.

Caustic soda is used as the main neutralization chemical in the process, which introduces sodium ions to the solution. The concentration of sodium and sulfate may be vastly higher than that of lithium, preventing the recovery of a pure lithium product. Glauber salt ($Na_2SO_4 \bullet 10H_2O$) is consequently crystallized from the solution through water evaporation before lithium recovery, which also raises the lithium concentration in the solution. The salt is separated from the solution by centrifugation or filtering. Lithium carbonate is precipitated by adding sodium carbonate to the solution and elevating the pH to 11 with caustic soda, and the formed lithium carbonate product is filtered or centrifuged from the solution, washed, and dried. The mother liquor is returned to the process to improve lithium recovery. All liquid effluent streams are subjected to final neutralization with lime milk to hydrolyze the dissolved metals as metal hydroxides and to form a gypsum cake.

The leaching step, copper cementation, and the recovery of cobalt, nickel, and lithium are the same in all the flowsheets. The scenarios are summarized as follows:

- *FS1:* Manganese, aluminum, and iron are extracted with D2EHPA after copper cementation and the raffinate is treated for cobalt recovery. Manganese is selectively stripped with sulfuric acid into a pure solution and recovered by oxidative precipitation, while iron and aluminum are scrubbed with strong hydrochloric acid solution and removed by neutralization.
- *FS2*: Iron and aluminum are removed directly by neutralization after copper cementation, and manganese is separated from the purified solution with D2EHPA and stripped. The raffinate is treated for cobalt recovery.
- *FS3*: Iron and aluminum are removed by neutralization after copper cementation as in *FS2*; manganese is not purified by solvent extraction but directly recovered by oxidative precipitation. The solution is treated for cobalt recovery.

The effect of decreasing the initial sulfuric acid concentration was studied only with flowsheet 2. The baseline conditions were 2 M initial sulfuric acid concentration, 1-h

residence time, an aqueous Fe/$LiMeO_2$ ratio of 0.11, and a solid Cu/2$LiMeO_2$ ratio of 1.2. The acidity, residence time, and final extractions were changed in the low acid (LA) system, and the rest of the flowsheet model was unchanged.

- *FS2-LA*: The sulfuric acid feed is controlled so that the final pH of the leaching solution is 1.89 after 92% cobalt is extracted with a residence time of 2 h. Nickel and manganese were assumed to dissolve at a similar rate to cobalt.

2.1.2 Functional unit and allocation procedure

The functional unit (FU) of the study was the *hydrometallurgical treatment of 1 kg black mass* in accordance with the goal statement. The process was scaled for a plant operating 8000 h annually with a capacity of 125,000 batteries, which represents the reported 2030 capacity of Northvolt's recycling facilities (Latini et al. 2022). Cathode and anode materials comprise approximately a quarter of the battery weight (Brückner et al. 2020), leading to a corresponding throughput of 4 tonnes per hour to the hydrometallurgical process. The processing was presumed to occur within Europe.

The substitution method was used to assess the net impacts of recycling against virgin raw material production using a 1:1 ratio to find an optimal solution between recovery and process conditions. This approach has been used in most studies regarding battery recycling (Dunn et al. 2012; Mohr et al. 2021; Raugei and Winfield 2019; Rajaeifar et al. 2021). The stoichiometric substitution was conducted only for the pure metal compound excluding the impurity content, but the further refining of intermediate precipitates will cause unaccounted burdens in the downstream, which is acknowledged. The purpose of assessing the avoided burdens was to address the trade-offs between maximizing valuable recoveries and minimizing chemical and energy consumption.

Due to the exclusion of pre-treatment from the system boundary, the study underestimates both the total process impacts and the benefits from the process. Several studies estimate that the pre-treatment steps are far less environmentally intensive than the subsequent processing stages (Kallitsis et al. 2022; Rajaeifar et al. 2021; Wu et al. 2022; Zhou et al. 2021), and the separation of copper and aluminum current collectors brings large benefits. Since pre-treatment processes vary substantially, the assumption that these stages have small impacts may not be justified in all cases, and conclusions should be drawn carefully about the comparison of recycling and virgin metals.

2.1.3 Impact assessment method

The CML v.4.8 (2016) midpoint method was used to quantify the environmental impacts. The environmental impact categories considered were the following: global warming (GWP, unit kg CO_2-eq), acidification (AP, unit kg SO_2-eq), freshwater eutrophication (EP, kg phosphate-eq), ozone depletion (ODP, kg R11-eq), and photochemical oxidant creation (POCP, kg ethene-eq). The selected categories are those recommended by Santero and Hendry (2016) for use in the assessment of mining and metallurgical products.

Although resource depletion and toxicity categories are deemed less robust, human toxicity (HTP, kg DCB-eq), abiotic depletion of elements (ADPe, kg Sb-eq), and abiotic depletion of fossil resources (ADPf, MJ) were also included. Toxic emissions and mineral resource depletion from metal extraction for batteries are predicted to increase due to electrification (Peters et al. 2017), which supports their inclusion in the assessment.

2.2 Life cycle inventory

The LCI was formulated around the process simulation, which provides very detailed information on the in- and outflows of the system. Literature and expert estimates were needed for some of the flows, which could not be obtained directly or reliably from the simulation.

2.2.1 Assumptions in inventory modeling

Some of the key assumptions in the inventory modeling stage are described below, but a more detailed account of the parameters used, and the HSC model are described in "Sections 1 and 2" of the Supplementary information (SI). The analysis is prospective, and no primary data of the process could therefore be obtained. The information on the foreground system was obtained by upscaling laboratory-scale units with process simulation. This is deemed suitable tool for LCI data generation in chemical engineering (Parvatker and Eckelman 2019), but it should be observed that the parameters selected from experimental literature may not be fully representative of the process on industrial scale. Villares et al. (2017) argued that prospective LCA is a different kind of tool to conventional LCA, and the results and implications of the study should be used to inform further hydrometallurgical process development rather than being accepted as the final outcome.

The advantage of the use of process simulation in the generation of data is that it does not rely on the modification of secondary LCI data from the literature. The model was built mainly with the "Reaction" type unit models in HSC, where the outputs of a process unit are calculated with chemical reactions, inputs, and phase distributions with the aid of parameter controls. The model is internally consistent since changes in an upstream process are also experienced in the downstream, but the parameters themselves have some uncertainty.

HSC Sim does not provide an estimate for the electricity consumption of the units, and the power consumption by the process was therefore calculated based on the dimensions of the main equipment: reactors, thickeners, filters, centrifuges, and crystallizers, with a 15% safety factor. Individual pumps, automation, lights, and other auxiliary equipment were not calculated, but instead included as a "general electricity constant," which was estimated at 1 MW per 10 tonnes of black mass and is equal between the scenarios. The power consumption was calculated in steady state and the throughput to the units was assumed to be unrelated to the residence time in other units, which is a definite potential source of error. Nevertheless, the estimated electricity consumption is based on physical relationships between the equipment dimensions and the simulation. Unexpected problems may arise in moving from laboratory to pilot to industrial scale.

The black mass used (Table 2) had a low copper and aluminum content and therefore was not "self-reducing," so copper had to be fed externally into the process. Although copper was circulated in the process flowsheet from cementation back to leaching, some losses are inevitable, so a small copper feed was needed to maintain the system. It was presumed that the copper feed in the LCI was scrap copper, preferably the copper foils recovered in pre-treatment. The leaching stage was modeled with copper rather than aluminum, which is a stronger reducing agent, because aluminum is a challenging impurity for hydrometallurgical circuits.

The process included several large solvent extraction systems for manganese, cobalt, and nickel. The study by Rinne et al. (2021) utilized a black-box approach where extraction and stripping are all modeled with a single unit, but this study included the organic compounds aside from the tributyl phosphate (TBP) modifier used in cobalt and nickel extraction. The extraction, organic scrubbing, and stripping units were modeled separately but in only one stage each. There were no datasets in Ecoinvent 3.8 for the extractants—D2EHPA

Table 2 LCI data for the investigated scenarios (FU = 1 kg processed black mass)

Inflows	***FS1***	***FS2***	***FS3***	***FS2-LA***	**Unit/FU**
Black mass	1.00	1.00	1.00	1.00	kg
Electricity, EU2020	1.66	1.60	1.53	1.45	MJ
Steam, chemical industry	5.22	4.54	4.68	4.59	MJ
Deionized water	11.75	8.97	7.68	8.37	kg
Sulfuric acid	2.90	2.81	2.72	1.58	kg
Caustic soda	1.91	1.74	1.75	0.79	kg
Lime, as quicklime	18.08	17.85	19.73	7.17	g
Sodium carbonate	184.22	180.85	180.89	170.42	g
Hydrochloric acid	126.86	-	-	-	g
Copper scrap	60.22	60.22	60.22	70.72	g
Iron scrap	71.09	71.09	71.09	67.66	g
Sulfur dioxide, liquid	1.68	1.64	1.93	1.50	g
Oxygen, liquid	54.87	51.15	57.23	45.64	g
Kerosene	1.15	1.03	0.55	1.00	kg
D2EHPA	0.14	0.15	0.08	0.14	kg
Cyanex 272	0.14	0.10	0.11	0.10	kg
Outflows	***FS1***	***FS2***	***FS3***	***FS2-LA***	**Unit**
Lithium carbonate	128.43	126.08	126.33	118.81	g
Cobalt sulfate heptahydrate	870.81	850.40	824.42	778.84	g
Nickel sulfate hexahydrate	126.67	123.51	121.40	113.88	g
Manganese dioxide	25.62	23.26	23.26	21.32	g
Solid wastes, non-salt	0.80	0.92	0.92	0.90	kg
Glauber salt waste	3.50	3.53	3.43	1.77	kg
Wastewater	12.43	8.96	10.07	15.87	kg
Sulfate to freshwater	63.97	45.84	71.09	30.75	g
Cobalt to freshwater	159.85	209.94	176.64	217.50	mg
Nickel to freshwater	31.76	38.26	31.73	37.43	mg
Copper to freshwater	0.22	0.28	0.27	0.20	mg

and Cyanex 272—so the approximate LCI provided by Cao et al. (2023) was used to model their production impacts. The organic phase is consumed through chemical degradation and crud formation, and the makeup is dependent on process specific factors and the extractant itself, and Cao et al. (2023) assumed that 5% of the organic phase is replaced. It was also assumed in this study that the input in the LCI is 5% of the total kerosene-extractant mixture in circulation.

Finally, the LCI data is only as reliable as the simulation model that is used to generate the data. The process simulation is only a simplification of a highly complex process, where each of the units may affect the subsequent units. For instance, not all interactions could be embedded into the leaching model: Chernyaev et al. (2021a) observed that dissolved copper may be cemented by metallic aluminum foils in the solution, which decreases the amount of dissolved copper. Another example of this would be that if the iron level in the leaching solution is higher than predicted, more cobalt and nickel could be lost to the iron- and aluminum-bearing neutralization residues, but the losses were presumed to be static in the model. The effect would be seen in the valuable metal recovery rates and the net impacts.

2.2.2 Inventory analysis

The life cycle inventory was compiled by normalizing all the in- and outflows in the simulation for the functional unit, 1 kg of treated black mass. Background data was obtained from the Ecoinvent 3.8 database, and the electricity production mix for the process was modeled after the EU reference scenario technology mix for 2020: 40% renewables, 25% nuclear, and the rest fossil carbon fuels (European Commission 2021). The compiled LCI data for each of the scenarios is provided in Table 2, and in more detail in Table S5.

3 Results and discussion

The study considered both the technical and the environmental aspects of hydrometallurgical black mass recycling to inform process development. Simulation results, including product purity and recoveries, copper and iron behavior, and waste streams are discussed in the SI, "Section 3" and further needs for experimental data are summarized in "Section 4" of the SI.

3.1 Scenario analysis

The process impacts and recovery credits are presented in Fig. 2. It was observed that *FS1* had the highest process impacts in all categories and *FS3* the lowest. The 100-year GWP for each of the scenarios was 7.96 kg CO_2-eq for FS1, 6.22 kg CO_2 eq for FS2, and 5.44 kg CO_2-eq for FS3 per FU. The largest differences between the scenarios were in ozone depletion and the smallest in acidification, and the *FS1* impacts were approximately 14–27% greater than for *FS2*, and 23–41% greater than for *FS3*. These differences do not appear inconsequential given their magnitude.

The final metal recoveries in *FS1*, *FS2*, and *FS3*, respectively, were 97.2%, 94.9%, and 92.0% for cobalt, 94.6%, 92.3%, and 91.0% for nickel, 87.4%, 85.2%, and 86.0% for lithium, and 97.1%, 94.8%, and 94.8% for manganese. In all but *FS1*, some of the valuable metals were incorporated into the iron-aluminum-bearing neutralization waste, while *FS3* saw some additional cobalt and nickel losses to the manganese dioxide product. The reason why lithium recovery was lower in *FS2* than *FS3* is most likely to do with solution volumes. The differences in valuable metal recoveries affect the metal credits. The model indicates that product purity would be a problem for manganese dioxide: < 99% in all scenarios and even < 70% in *FS3*, and a possible issue for lithium carbonate, < 99% in *FS3*. Lithium carbonate, and nickel and cobalt sulfates can be refined further by a simple re-crystallization process. Manganese dioxide is not water soluble and requires reductive leaching to further refine it, although the process is not overly complex or multi-step.

The process impacts were lower than the total of primary nickel, cobalt, lithium, and manganese chemical production in all but ozone depletion in *FS1*, where the net impacts were + 9.42E-7 kg R11-Eq. (34% higher than virgin metals) despite the highest metal recoveries. In *FS2*, the ODP was only negligibly (− 0.6%) lower in the recycling process, but the difference was larger in *FS3* (− 16.2%). Recycling benefited ADPe (approximately − 97% to − 98% between the scenarios) and HTP (~ 90%) the most significantly, which is consistent with the fact that the toxicity and mineral depletion impacts of EVs are typically predicted to be higher than those of ICEVs (Mendoza Beltran et al. 2018; Helmers et al. 2020; Arshad et al. 2022).

The recycling credits were overwhelmingly from cobalt sulfate recovery, as shown in Fig. 2. This was due to two factors: cobalt was the main battery metal in the black mass (Table 1), and the most intensive of them to produce based on the data used for virgin or market metals. The recovery of lithium carbonate and nickel sulfate appeared beneficial considering the low content of both metals, while the credits for manganese dioxide were significantly less.

The credits are dependent on the data source. For instance, the GWP of the recycling process was 23% (*FS2-LA*) to 35% (*FS1*) of the virgin impacts using Ecoinvent 3.8 values for cobalt sulfate, while using Cobalt Institute's (2022) data made recycling appear far less environmentally sound, as only *FS2-LA* led to any benefits in GWP (− 6%). The recycling credits are not static, however, and a future-oriented assessment should also consider the effects of decarbonization and falling ore grades on the primary

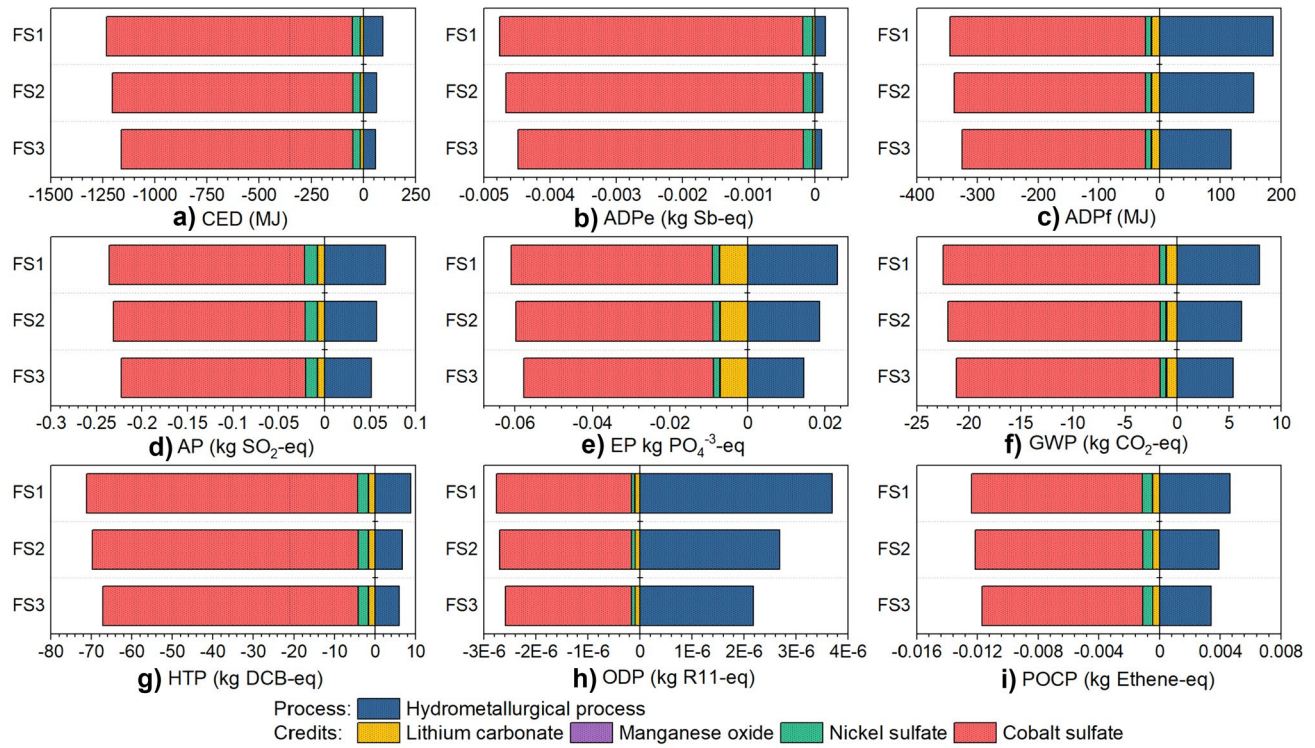

Fig. 2 Impact characterization for the process per FU (1 kg black mass). **a** CED, MJ; **b** ADPe, kg Sb-eq; **c** ADPf, MJ; **d** AP, kg SO_2-eq; **e** EP, kg phosphate-eq; **f** GWP, kg CO_2-eq; **g** HTP, kg DCB-eq; **h** ODP, kg R11-eq; **i** POCP, kg ethene-eq

routes and background processes (Harpprecht et al. 2021; Šimaitis et al. 2023). However, considering the boundaries, they were not relevant in this work.

While the above example highlights that the comparison of recycling to virgin production may be misleading, it can nevertheless be useful in determining the optimal solution between valuable metal recovery and process conditions. *FS1* had the highest recoveries for each of the metals, but this was offset by the increased process intensity in all but ADPe. *FS3*, on the other hand, had the lowest impacts but also the lowest nickel and cobalt recovery and therefore the lowest net impacts (Fig. 3, i.e., after factoring in the recovery credits) in ADPf, EP, ODP, and POCP. *FS2* provided a balance between the two scenarios, and it was the preferred option in terms of CED, AP, GWP, HTP, and the second after *FS1* in ADPe.

It is likely that the impacts of *FS1* are underestimated in the model, as the presence of aluminum and iron in the manganese SX circuit as well as the harsh stripping conditions should theoretically lead to crud formation and a faster rate of organic degradation. The SX process suggested by Peng et al. (2019) is an interesting one, but it is technically difficult to implement as is. Whereas the technical and environmental issues of *FS1* appear clear, the results were more ambiguous between *FS2* and *FS3*. Given that *FS2* seemed to be a compromise solution between overall recovery and process impacts, it was selected for further assessment. However, both options have their merits.

The recovery of impure lithium, manganese, cobalt, or nickel intermediates that can be integrated into existing processes is a possible way to streamline the flowsheets, as in the case of manganese dioxide in *FS3*. This would bring additional refining impacts from further refining, the effects of which are unknown.

The low acid leaching scenario (*FS2-LA*) was analyzed with the *FS2* flowsheet for simplicity, see Fig. 4. The pH after leaching was 1.89. The leaching extractions were lower than in the baseline conditions despite the twice as long residence time in leaching (higher power consumption in leaching), and the estimated final recoveries were 80.9% lithium, 86.3% cobalt, 83.1% nickel, and 86.4% manganese. The stage-specific LCI (Table S5) showed that copper scrap consumption increased. This was related to the dynamics in the reactions between lithium metal oxides, iron, and copper in the model—less ferric iron was available to oxidize copper due to the decreased lithium metal oxide dissolution. Although interesting, the finding was assumed inconsequential for the LCA results.

The decrease in acidity, as evident in Fig. 4, reduced each of the process impacts quite significantly. The decrease was not only due to sulfuric acid but also from downstream consumption of neutralizing chemicals. The 100-year GWP of

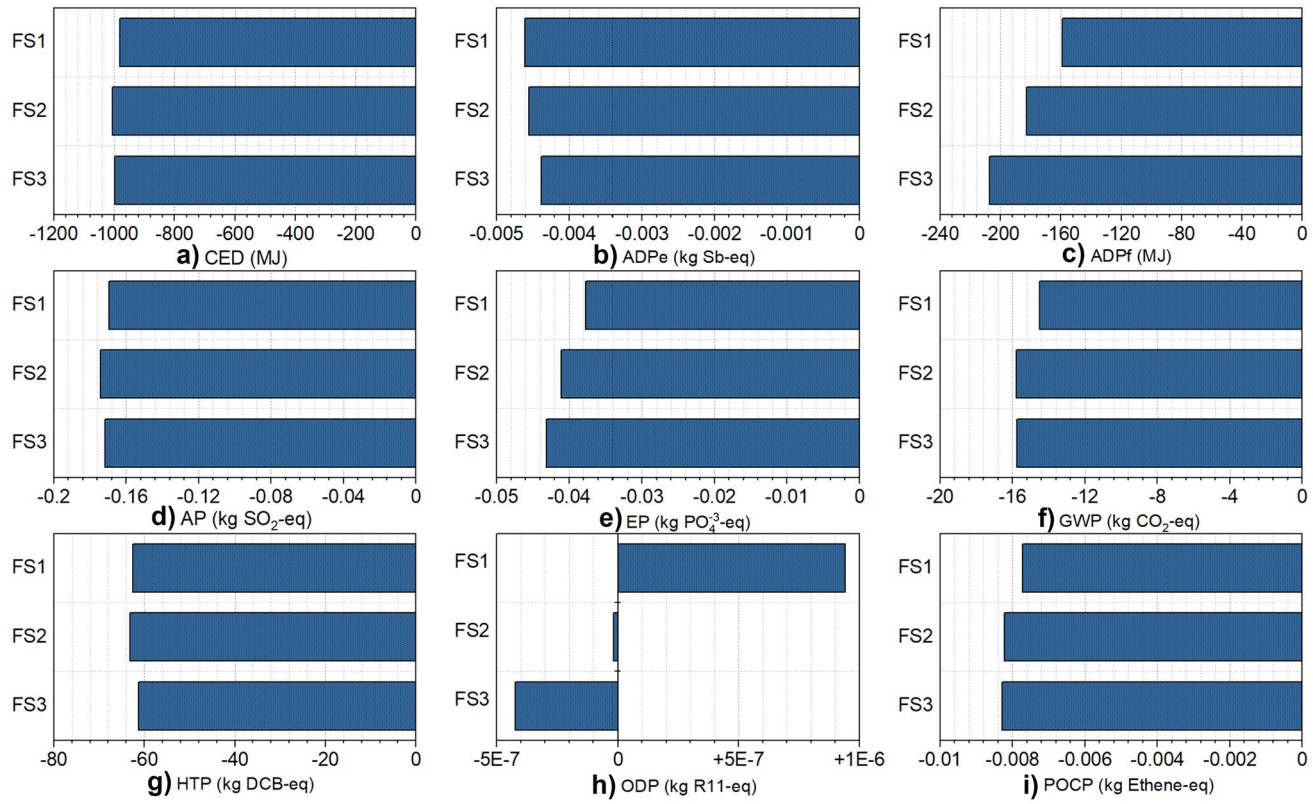

Fig. 3 Net impacts of the scenarios after factoring in both the process and the credits. **a** CED, MJ; **b** ADPe, kg Sb-eq; **c** ADPf, MJ; **d** AP, kg SO_2-eq; **e** EP, kg phosphate-eq; **f** GWP, kg CO_2-eq; **g** HTP, kg DCB-eq; **h** ODP, kg R11-eq; **i** POCP, kg ethene-eq

the low acid process was 4.42 kg CO_2-eq/FU, which was 20.1% of the equivalent virgin production. The milder leaching conditions affected GWP the least (− 28.8%) and ODP the most (− 44.2%). Although the *FS2-LA* system had considerably lower valuable metal extractions than the baseline *FS2*, the net impacts of *LA* scenario were also lower in all categories, but the gap was significantly smaller when the net was compared against process impacts. ADPe was the most sensitive category to recovery, and the difference between the net impacts of the scenarios was only 1.1%. The net ODP, in contrast, decreased 70-fold.

The results indicate that the optimization of leaching would be beneficial despite some valuable metal losses and an increase in residence time, which affects power consumption and reactor size. The analysis was also based on a single experimental study, and there is further potential for improving the leaching extraction at a higher final pH.

3.2 Contribution analysis

The contribution analyses (Fig. 5) demonstrate clearly that the neutralization and SX processes were by far the largest contributors to the process. The organics (Cyanex 272, D2EHPA, and kerosene together, GWP 56.2–82.4%), caustic soda (GWP 10.4–19.2%), and sulfuric acid (GWP 2.2–3.8%) are the most significant individual flows, even in *FS3,* which avoids the need for a manganese solvent extraction system. All of the chemicals mentioned were consumed in SX, which explains the findings.

The process has only minor foreground impacts (direct emissions) in HTP from the minor amount of metal emissions to water, which contributes < 1% of total HTP between the scenarios and is counted towards effluent treatment. The process is not energy-intensive as seen from Fig. 5b, but steam consumption by the crystallizers is observable in GWP, especially for *FS3* (9.0%). Copper scrap is associated with a very small credit (largest for HTP, − 0.4 to 1.0%) due to its modeling in the database, and copper and iron consumption in the process appear to have a negligible effect on anything other than negating the need for other reducing agents.

Although leaching in and of itself contributes substantially only to AP (~ 30% *FS1-FS3*, 16.9% *FS2-LA*) and POCP (~ 20% *FS1-3*, 9.2% *FS2-LA*) mainly due to sulfuric acid consumption, the effect of leaching is also felt downstream in the process as can be observed by comparing *FS2* and *FS2-LA*. The consumption of caustic soda is effectively reduced in iron and aluminum removal by performing the

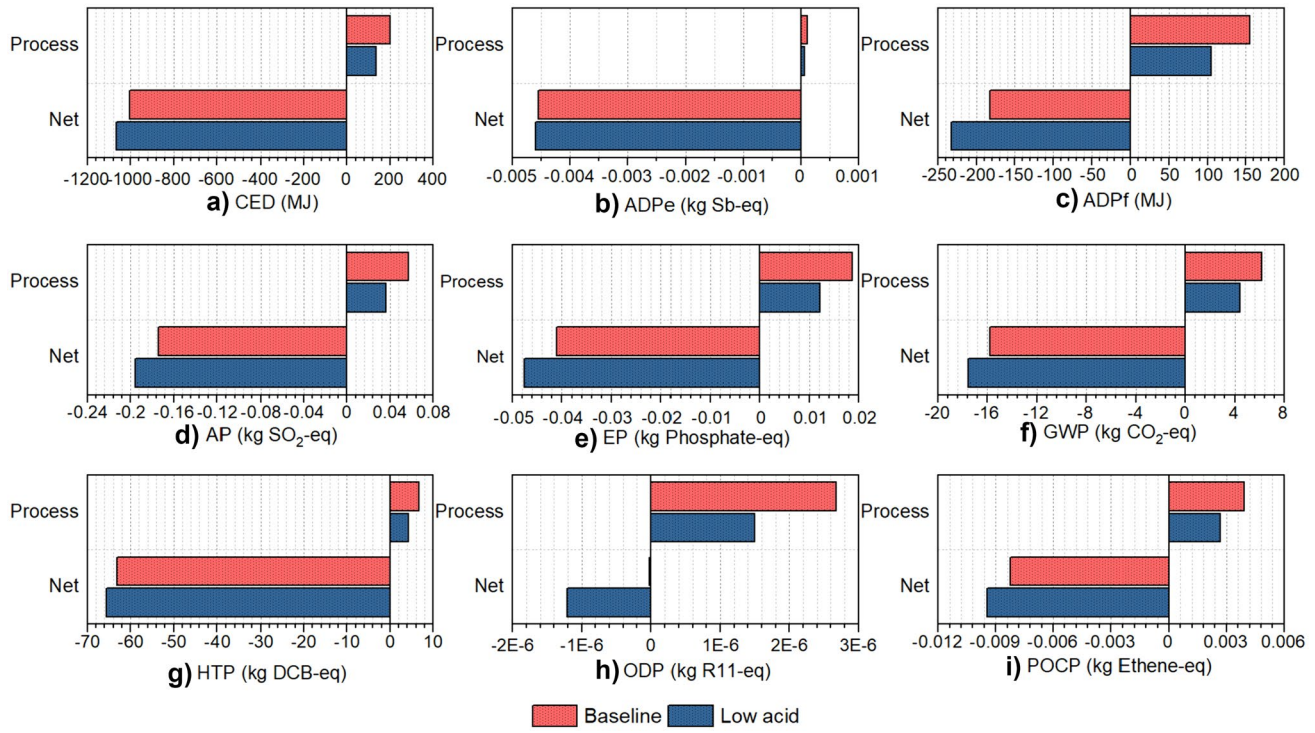

Fig. 4 Comparison of *FS2* impacts between low and baseline leach solution acidity, both process and net impacts per FU. **a** CED, MJ; **b** ADPe, kg Sb-eq; **c** ADPf, MJ; **d** AP, kg SO_2-eq; **e** EP, kg phosphate-eq; **f** GWP, kg CO_2-eq; **g** HTP, kg DCB-eq; **h** ODP, kg R11-eq; **i** POCP, kg ethene-eq

leaching step in milder conditions. The reduction in caustic soda use is, based on the contributions, more significant than the lower consumption of sulfuric acid particularly for ODP, but also GWP, CED, ADPe, ADPf, EP, and HTP impacts.

An interesting finding in this study is that leaving out the organic chemicals used in SX is probably not justifiable, yet only few metallurgical studies transparently report the modeling of SX chemicals (Arshi et al. 2018; Bailey et al. 2021; Liu and Keoleian 2020; Vahidi and Zhao 2017). The issue of lacking representative database data for the organics has also been noted by Cao et al. (2023) and Vahidi and Zhao (2017). The studied process had three SX systems, and the amount of replaced organics was substantial, despite the re-use of the organic phase based on the simulation, and the LCIA model is presumed to be sensitive to the consumption of makeup organics (assumed 5% of all organics in circulation). The effect of changing the assumed value is quite clear without additional analysis—higher consumption would make *FS3* more advantageous, while lower consumption would reduce the gap between *FS3* and the other scenarios.

The consumption of organics, acid, and caustic soda may also theoretically be reduced by decreasing the solution volume through increasing the solid-to-liquid (S/L) ratio in leaching. The S/L ratio assumed in the leaching step of this study was 1:10, but the literature indicates that 1:5 is likely to be viable with otherwise comparable leaching conditions (Chernyaev et al. 2021a). The challenge with this approach is that the leaching reactions are acid-consuming, and increasing the solids concentration does not change this. Furthermore, it may be challenging to treat highly concentrated metal solutions by SX, and the practical effects should be evaluated experimentally before implementation in the model.

3.3 Sensitivity to NMC black masses

The black mass composition (Table 1) was changed to assess the sensitivity of the LCI flows and therefore also the impacts to the input. NMC chemistries, which dominate the EV markets, were selected for the analysis, which was conducted with *FS2*. The black mass compositions were calculated so that the impurities were kept constant and only the molar ratios of the oxides $LiCoO_2$, $LiNiO_2$, and $LiMnO_2$ were changed.

The calculations showed (Fig. 6) that changes in the black mass chemistry increased the process impacts in all categories aside from abiotic element depletion, where NMC111 resulted in − 0.6% reduction. NMC532 led to the largest and NMC811 to the smallest change from the default cobalt-rich chemistry, so the variation appears to be related to the manganese content in the black mass. The precipitation of manganese consumed oxygen and sulfur dioxide proportionately to its content in the

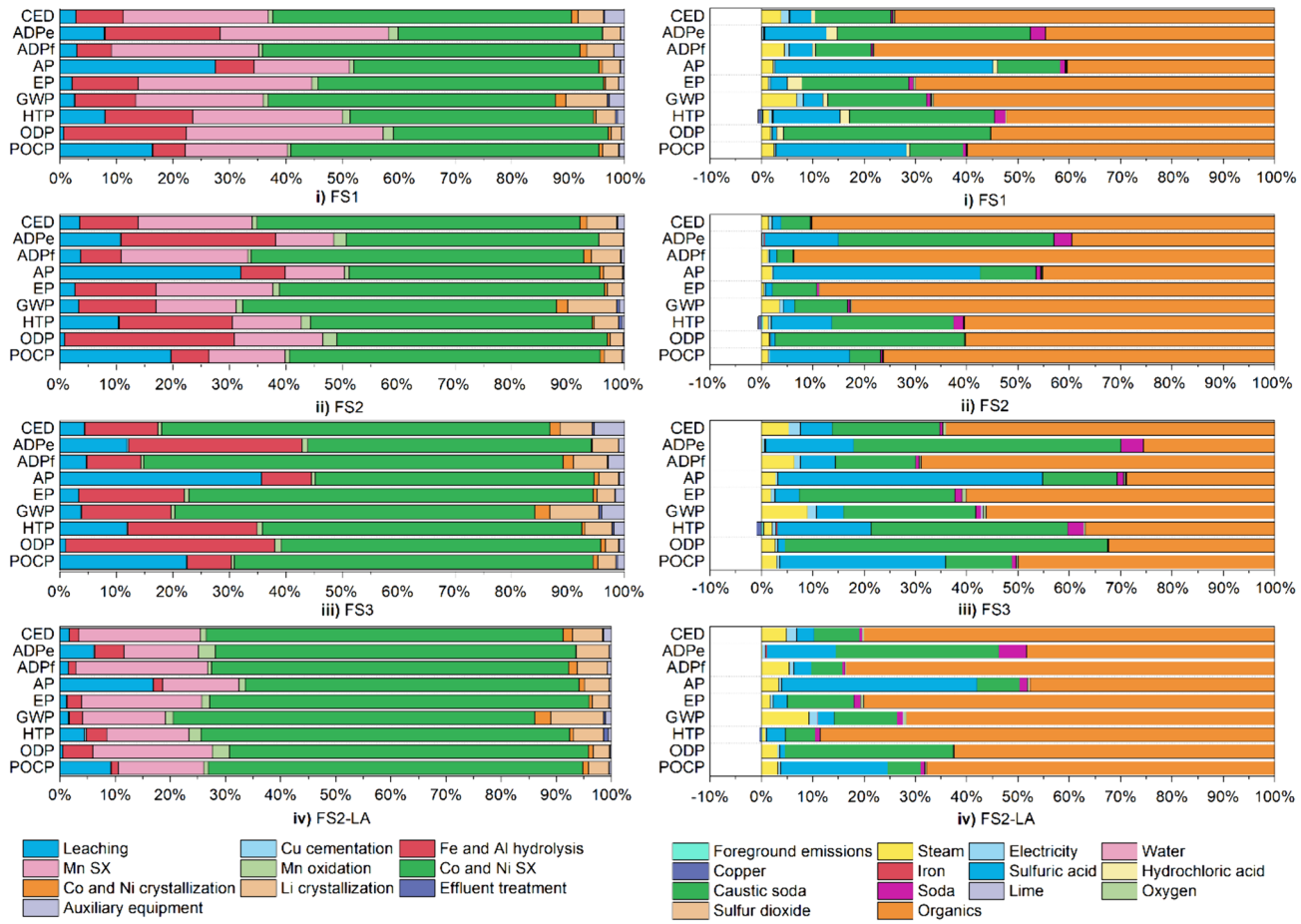

Fig. 5 **a** Contribution analysis on process unit level in each scenario. **b** Contribution analysis on flow level. (i) *FS1*. (ii) *FS2*. (iii) *FS3*. (iv) *FS2-LA*

black mass, as evident from Table S6, and appeared to slightly affect the consumption of energy and organics.

Even the largest differences observed in human toxicity were only + 3.1%, + 3.1%, and + 1.2% for NMC111, 532, and 811, respectively. In terms of GWP, the impacts increased by 2.5%, 2.8%, and 1.4% for each of the studied chemistries in the same order, and the average difference from the default *FS2* was 1.8%, 2.0%, and 0.8%. The differences are, therefore, not substantial, and the effect of the cathode active material composition is limited to certain consumables when the impurities and inert carbon are kept constant. This is only true for black masses containing cobalt, nickel, and manganese, however, and a major shortcoming of the process is that it is not tailored to process LFP batteries efficiently. LFP cathodes could, at best, provide reducing power for the leaching step through iron, and dissolved lithium can be recovered, but the iron and phosphate would be lost.

Overall, the findings from the scenario and sensitivity analyses suggest that the black mass composition mainly affects the recovery units and is not as critical as the process parameters. The optimization of leaching conditions was recognized to have a major effect on downstream chemical consumption, but this observation is intuitively quite universal for all hydrometallurgical processing, particularly in acidic media.

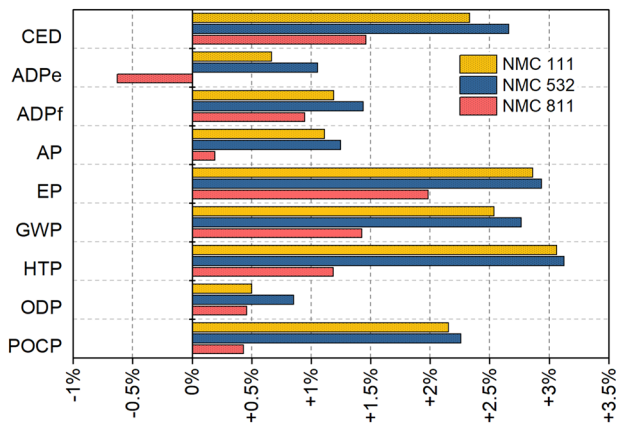

Fig. 6 Change in the process impacts from the Co-rich baseline using *FS2* simulation model (± %)

4 Conclusions

A detailed LCA of hydrometallurgical battery recycling was undertaken to understand the connections between process parameters, flowsheet configurations, and the environmental impacts of the process. The study suggests that hydrometallurgical material recovery leads to significant benefits across all the considered impact categories, including ozone depletion, provided that the leaching parameters are optimized. Recommendations for further process development can be made based on the technical and environmental performance of the different scenarios, and the study has been used to guide further research needs.

The results of this study suggest that research efforts should focus on optimizing sulfuric acid consumption in leaching. Modeling the leaching step with a final PLS of pH 1.9 rather than with the initial 180 g/L sulfuric acid decreased the global warming impacts of the process from 6.22 to 4.42 kg CO_2-eq, and the net impacts after factoring in the credits from − 15.79 to − 17.58 CO_2-eq for a 1-kg black mass. The acidity affected not only the sulfuric acid consumption, but also that of caustic soda. In contrast, the black mass composition had only a small effect on the impacts through the share of manganese in the feed. The third significant finding was that the organic chemicals used in solvent extraction contributed significantly to the impacts despite their re-use in the process, which shows that SX chemicals should not be ignored outright due to the lack of primary LCI data. In fact, this study indicates the need for LCI data on the common extractants used in metal processing.

The recovery of manganese has received less attention than that of nickel, cobalt, or lithium, and technically established methods are still lacking. Solvent extraction could be a selective way to purify manganese solution while avoiding nickel and cobalt losses, although this would lead to a complex flowsheet with environmentally burdensome pH control, at the expense of purity. It should, however, be kept in mind that the process was scaled to industrial from laboratory scale using process simulation, and further experimental and pilot work would be required to validate the model.

The limitation of the study is that it only considers the prospective future impacts of hydrometallurgical black mass recycling. While pre-treatment is its own entity, combining the two steps would be beneficial to see the pack level impacts. From a metallurgical and process perspective, it is important that the black mass entering a hydrometallurgical circuit would be low in aluminum to avoid processing challenges. Additionally, the study did not consider cost or social aspects, which are both vital for holistic sustainability.

Further process development should focus on the optimization of the leaching conditions to minimize downstream consumption of chemicals, while pre-treatment should aim to efficiently reject aluminum from the feed to the hydrometallurgical process. The benefit of using copper and iron as reducing agents are not obvious from the LCA without thorough comparison with hydrogen peroxide-based systems, but the simulation showed that even low copper contents in the black mass may be enough if recovered for re-use. The recovery of previously under-researched metals and materials, like graphite, manganese, and aluminum, should be made a priority.

Supplementary Information The online version contains supplementary material available at https://doi.org/10.1007/s11367-024-02304-y.

Funding Open Access funding provided by Aalto University. This study was supported by BATCircle 2.0 (grant number 44886/31/2020), financed by Business Finland, and the School of Chemical Engineering at Aalto University. The Academy of Finland's RawMatTERS Finland Infrastructure (RAMI) and interaction with the Horizon Europe-funded RESPECT project (grant agreement 101069865) are also gratefully acknowledged.

Data availability All data generated or analyzed during this study is included in this published article and its supplementary information files. Further details about the simulation are available from the corresponding author upon reasonable request.

Declarations

Competing interests The authors declare no competing interests.

References

Andre D, Kim S, Lamp P, Lux SF, Maglia F, Paschos O, Stiaszny B (2015) Future generations of cathode materials: an automotive industry perspective. J Mater Chem A 3:6709–6732. https://doi.org/10.1039/C5TA00361J

Arshad F, Lin J, Manurkar N, Fan E, Ahmad A, Tariq M, Wu F, Chen R, Li L (2022) Life cycle assessment of lithium-ion batteries: a critical review. Resour Conserv Recycl. https://doi.org/10.1016/j.resconrec.2022.106164

Arshi PS, Vahidi E, Zhao F (2018) Behind the scenes of clean energy: the environmental footprint of rare earth products. ACS Sus Chem Eng 6:3311–3320. https://doi.org/10.1021/acssuschemeng.7b03484

Bailey G, Orefice M, Sprecher B, Önal MAR, Herraiz E, Dewulf W, Van Acker K (2021) Life cycle inventory of samarium-cobalt permanent magnets, compared to neodymium-iron-boron as used in electric vehicles. J Clean Prod. https://doi.org/10.1016/j.clepro.2020.125294

Bauer C, Hofer J, Althaus HJ, Del Duce A, Simons A (2015) The environmental performance of current and future passenger vehicles: life cycle assessment based on a novel scenario analysis framework. Appl Energy 157:871–883. https://doi.org/10.1016/j.apenergy.2015.01.019

Bicer Y, Dincer I (2018) Life cycle environmental impact assessments and comparisons of alternative fuels for clean vehicles. Resour Conserv Recycl 132:141–157. https://doi.org/10.1016/j.resconrec.2018.01.036

Blömeke S, Scheller C, Cerdas F, Thies C, Hachenberger R, Gonter M, Herrmann C, Spengler TS (2022) Material and energy flow analysis for environmental and economic impact assessment of industrial recycling routes for lithium-ion traction batteries. J Clean Prod. https://doi.org/10.1016/j.jclepro.2022.134344

Brückner L, Frank J, Elwert T (2020) Industrial recycling of lithium-ion batteries – a critical review of metallurgical process routes. Metals. https://doi.org/10.3390/met10081107

Cao Y, Li L, Zhang Y, Liu Z, Wang L, Wu F, You J (2023) Co-products recovery does not necessarily mitigate environmental and economic tradeoffs in lithium-ion battery recycling. Resour Conserv Recycl. https://doi.org/10.1016/j.resconrec.2022.106689

Chernyaev A, Partinen J, Klemettinen L, Wilson BP, Jokilaakso A, Lundström M (2021a) The efficiency of scrap Cu and Al current collector materials as reductants in LIB waste leaching. Hydrometallurgy. https://doi.org/10.1016/j.hydromet.2021.105608

Chernyaev A, Wilson BP, Lundström M (2021b) Study on valuable metal incorporation in the Fe-Al precipitate during neutralization of LIB leach solution. Sci Rep. https://doi.org/10.1038/s41598-021-02019-2

Chernyaev A, Zou Y, Wilson BP, Lundström M (2022) The interference of copper, iron and aluminum with hydrogen peroxide and its effects on reductive leaching of $LiNi_{1/3}Mn_{1/3}Co_{1/3}O_2$. Sep Purif Technol. https://doi.org/10.1016/j.seppur.2021.119903

Chu B, Guo Y, Shi J, Lin Y, Huang T, Su H, Yu A, Guo Y, Li Y (2022) Cobalt in high-energy-density layered cathode materials for lithium ion batteries. J Power Sources. https://doi.org/10.1016/j.jpowsour.2022.231873

Ciez R, Whitacre JF (2019) Examining different recycling processes for lithium-ion batteries. Nat Sustain 2:148–156. https://doi.org/10.1038/s41893-019-0222-5

Cobalt Institute (2022) Life cycle assessment of cobalt products. https://www.cobaltinstitute.org/sustainability/cobalt-sulphate/. Accessed 3 Apr 2024

Commission E (2021) EU Reference Scenario 2020: Energy, transport and GHG emissions – Trends to 2050. Publications Office. https://doi.org/10.2833/35750

Dunn JB, Gaines L, Sullivan J, Wang MQ (2012) Impact of recycling on cradle-to-gate energy consumption and greenhouse gas emissions of automotive lithium-ion batteries. Environ Sci Technol 46:12704–12710. https://doi.org/10.1021/es302420z

Ecoinvent (2021) Ecoinvent v3.8. Available at: https://ecoinvent.org/the-ecoinvent-database/data-releases/ecoinvent-3-8/. Accessed 15 Sep 2023

Faria R, Marques P, Moura P, Freire F, Delgado J, de Almeida AT (2013) Impact of the electricity mix and use profile in the life-cycle assessment of electric vehicles. Renew Sust Energy Rev 24:271–287. https://doi.org/10.1016/j.rser.2013.03.063

Guimarães LF, Botelho AB, Espinosa DCR (2022) Sulfuric acid leaching of metals from waste Li-ion batteries without using reducing agent. Min Eng. https://doi.org/10.1016/j.mineng.2022.107597

Harper G, Sommerville R, Kendrick E, Driscoll L, Slater P, Stolkin R, Walton A, Christensen P, Heidrich O, Lambert S, Abbott A, Ryder K, Gaines L, Anderson P (2019) Recycling lithium-ion batteries from electric vehicles. Nature 575:75–86. https://doi.org/10.1038/s41586-019-1682-5

Harpprecht C, van Oers L, Northey SA, Yang Y, Steubing B (2021) Environmental impacts of key metals' supply and low-carbon technologies are likely to decrease in the future. J Ind Ecol 25:1543–1559. https://doi.org/10.1111/jiec.13181

Helmers E, Dietz J, Weiss M (2020) Sensitivity analysis in the life-cycle assessment of electric vs. combustion engine cars under approximate real-world conditions. Sustainability. https://doi.org/10.3390/su12031241

ISO 14040:2006/A1:2020:en (2020) Environmental management – life cycle assessment, principles, and framework. Amendment 2 (ISO 14040:2006/Amd 1:2020)

Jiang S, Hua H, Zhang L, Liu X, Wu H, Yuan Z (2022) Environmental impacts of hydrometallurgical recycling and reusing for manufacturing of lithium-ion traction batteries in China. Sci Total Environ. https://doi.org/10.1016/j.scitotenv.2021.152224

Joulié M, Billy E, Laucournet R, Meyer D (2017) Current collectors as reducing agent to dissolve active materials of positive electrodes from Li-ion battery wastes. Hydrometallurgy 169:426–432. https://doi.org/10.1016/j.hydromet.2017.02.010

Kallitsis E, Korre A, Kelsall GH (2022) Life cycle assessment of recycling options for Li-ion batteries. J Clean Prod. https://doi.org/10.1016/j.jclepro.2022.133636

Keramidas K, Diaz Vazquez A, Weitzel M, Vandyck T, Tamba M, Tchung-Ming S, Soria-Ramirez A, Krause J, Van Dingenen R, Chai Q, Fu S, Wen X (2020) Global energy and climate outlook 2019: electrification for the low-carbon transition – the role of electrification in low-carbon pathways, with a global and regional focus on EU and China. Publications Office of the European Union, Luxembourg. https://doi.org/10.2760/350805

Latini D, Vaccari M, Lagnoni M, Orefice M, Mathieux F, Huisman J, Tognotti L, Bertei A (2022) A comprehensive review and classification of unit operations with assessment of outputs quality in lithium-ion battery recycling. J Pow Sour. https://doi.org/10.1016/j.jpowsour.2022.231979

Liu F, Peng C, Porvali A, Wang Z, Wilson BP, Lundström M (2019) Synergistic recovery of valuable metals from spent nickel-metal hydride batteries and lithium-ion batteries. ACS Sustain Chem Eng 7:16103–16111. https://doi.org/10.1021/acssuschemeng.9b02863

Liu L, Keoleian GA (2020). LCA of rare earth and critical metal recovery and replacement decisions for commercial lighting waste management. https://doi.org/10.1016/j.resconrec.2020.104846

Mendoza Beltran A, Cox B, Mutel C, van Vuuren DP, Vivanco DF, Deetman S, Edelenbosch OY, Guinée J, Tukker A (2018) When the background matters: using scenarios from integrated assessment models in prospective life cycle assessment. J Ind Ecol 1:64–79. https://doi.org/10.1111/jiec.12825

Metso (2023) HSC Chemistry Software. Available at: https://www.hsc-chemistry.com/. Accessed 14 Sep 2023

Mohr M, Peters JF, Baumann M, Weil M (2020) Toward a cell-chemistry specific life cycle assessment of lithium-ion battery recycling processes. J Indust Ecol 24:1310–1322. https://doi.org/10.1111/jiec.13021

Mohr M, Peters JF, Baumann M, Weil M (2021) Toward a cell-chemistry specific life cycle assessment of lithium-ion battery recycling processes. J Ind Ecol. https://doi.org/10.1111/jiec.13021

Nan J, Han D, Zuo X (2005) Recovery of metal values from spent lithium-ion batteries with chemical deposition and solvent extraction. J Power Sources 152:278–284. https://doi.org/10.1016/j.jpowsour.2005.03.134

Parvatker AG, Eckelman MJ (2019) Comparative evaluation of chemical life cycle inventory generation methods and implications for

life cycle assessment results. ACS Sustain Chem Eng 7:350–367. https://doi.org/10.1021/acssuschemeng.8b03656

Peng C, Chang C, Wang Z, Wilson BP, Liu F, Lundström M (2019) Recovery of high-purity MnO_2 from the acid leaching solution of spent Li-ion batteries. JOM 72:790–799. https://doi.org/10.1007/s11837-019-03785-1

Peters JF, Baumann M, Zimmermann B, Braun J, Weil M (2017) The environmental impact of Li-ion batteries and the role of key parameters – a review. Renew Sust Energy Rev 67:491–506. https://doi.org/10.1016/j.rser.2016.08.039

Porvali A, Aaltonen M, Ojanen S, Velazquez-Martinez O, Eronen E, Liu F, Wilson BP, Serna-Guerrero R, Lundström M (2019) Mechanical and hydrometallurgical processes in HCl media for the recycling of valuable metals from Li-ion battery waste. Resour Conserv Recycl 142:257–266. https://doi.org/10.1016/j.resconrec.2018.11.023

Porvali A, Chernyaev A, Shukla S, Lundström M (2020a) Lithium ion battery active material dissolution kinetics in Fe(II)/Fe(III) catalyzed Cu-H_2SO_4 leaching system. Sep Purif Technol. https://doi.org/10.1016/j.seppur.2019.116305

Porvali A, Shukla S, Lundström M (2020b) Low-acid leaching of lithium-ion battery active materials in Fe-catalyzed Cu-$H2_SO_4$ system. Hydrometallurgy. https://doi.org/10.1016/j.hydromet.2020.105408

Quan J, Zhao S, Song D, Wang T, He W, Li G (2022) Co-products recovery does not necessarily mitigate environmental and economic tradeoffs in lithium-ion battery recycling. Sci Total Environ. https://doi.org/10.1016/j.scitotenv.2022.153105

Rajaeifar MA, Raugei M, Steubing B, Hartwell A, Anderson PA, Heidrich O (2021) Life cycle assessment of lithium-ion battery recycling using pyrometallurgical technologies. J Indust Ecol 25:1560–1571. https://doi.org/10.1111/jiec.13157

Raugei M, Winfield P (2019) Prospective LCA of the production and EoL recycling of a novel type of Li-ion battery for electric vehicles. J Clean Prod 213:926–932. https://doi.org/10.1016/j.jclepro.2018.12.237

Rinne M, Elomaa H, Porvali A, Lundström M (2021) Simulation-based life cycle assessment for hydrometallurgical recycling of mixed LIB and NiMH waste. Resour Conserv Recycl. https://doi.org/10.1016/j.resconrec.2021.105586

Santero N, Hendry J (2016) Harmonization of LCA methodologies for the metal and mineral industry. Int J Life Cycle Assess 21:1543–1553. https://doi.org/10.1007/s11367-015-1022-4

Schade W, Haug I, Berthold D (2022) The future of automotive sector: Emerging battery value chains in Europe. https://doi.org/10.2139/ssrn.4220540

Šimaitis J, Allen S, Vagg C (2023) Are future recycling benefits misleading? Prospective life cycle assessment of lithium-ion batteries. J Ind Ecol 27:1291–1303. https://doi.org/10.1111/jiec.13413

Sphera (2022) GaBi solutions. Available at: https://sphera.com/product-sustainability-software/. Accessed 19 Sep 2023

Thompson DL, Hartley JM, Lambert SM, Shiref M, Harper GDJ, Kendrick E, Anderson P, Ryder KS, Gaines L, Abbott AP (2020) The importance of design in lithium-ion battery recycling – a critical review. Green Chem 22:7585–7603. https://doi.org/10.1039/D0GC02745F

Tsalidis GA, Korevaar G (2022) Environmental assessments of scales: The effect of ex-ante and ex-post data on life cycle assessment of wood torrefaction. Resources Resour Conserv Recycl. https://doi.org/10.1016/j.resconrec.2021.105906

Vahidi E, Zhao F (2017) Environmental life cycle assessment on the separation of rare earth oxides through solvent extraction. J Environ Manage 203:255–263. https://doi.org/10.1016/j.jenvman.2017.07.076

Vieceli N, Reinhardt N, Ekberg C, Petranikova M (2021) Optimization of manganese recovery from a solution based on lithium-ion batteries by solvent extraction with D2EHPA. Metals 11:1. https://doi.org/10.3390/met11010054

Villares M, Işildar A, van der Giesen C, Guinée J (2017) Does ex ante application enhance the usefulness of LCA? A Case Study on an Emerging Technology for Metal Recovery from e-Waste, Int J Life Cycle Assess 22:1618–1633. https://doi.org/10.1007/s11367-017-1270-6W

Wu F, Li L, Crandon L, Cao Y, Cheng F, Hicks A, Zheng EY, You J (2022) Environmental hotspots and greenhouse gas reduction potential for different lithium-ion battery recovery strategies. J Clean Prod. https://doi.org/10.1016/j.jclepro.2022.130697

Yao Y, Zhu M, Zhao Z, Tong B, Fan Y, Hua Z (2018) Hydrometallurgical processes for recycling spent lithium-ion batteries: a critical review. ACS Sustain Chem Eng 6:13611–13627. https://doi.org/10.1021/acssuschemeng.8b03545

Zhang W, Cheng CY (2007) Manganese metallurgy review. Part II: Manganese Separation and Recovery from Solution, Hydrometallurgy 89:160–177. https://doi.org/10.1016/j.hydromet.2007.08.009

Zhang P, Singh DM (2002) Oxidative precipitation of manganese with SO_2/O_2 and separation from cobalt and nickel. Hydrometallurgy 63:127–135. https://doi.org/10.1016/S0304-386X(01)00205-5

Zhou Z, Lai Y, Peng Q, Li J (2021) Comparative life cycle assessment of merging recycling methods for spent lithium ion batteries. Energies. https://doi.org/10.3390/en14196263